ELSEVIER

Journal of Alloys and Compounds 446–447 (2007) 157–161

Journal of ALLOYS AND COMPOUNDS

www.elsevier.com/locate/jallcom

Hydrogen absorption properties of the γ-$Mg_{17}Al_{12}$ phase and its Al-richer domain

J.-C. Crivello [a,*], T. Nobuki [a], S. Kato [b], M. Abe [c], T. Kuji [d]

[a] *School of High Technology for Human Welfare, Tokai University, Japan*
[b] *Department of Energy Science and Engineering, School of Engineering, Tokai University, Japan*
[c] *R&D Department, Nasu Denki-Tekko Co., Ltd. Koto-ku, Tokyo 136-0075, Japan*
[d] *Courses of Materials Science and Chemistry Unified Graduate School, Tokai University, 317 Nishino, Numazu-city, Shizuoka 410-0395, Japan*

Received 27 October 2006; received in revised form 12 December 2006; accepted 13 December 2006
Available online 21 December 2006

Abstract

In order to modulate the thermodynamic properties of the (Mg–Al)–H_2 system, the extended homogeneity range of the γ –$Mg_{17}Al_{12}$ intermetallic phase has been studied in Al-richer domain. In this paper, the two compounds at the nominal composition Mg_XAl_{100-X}, $X = 50$ and 58.6 are presented.

The samples were prepared by the bulk mechanical alloying (BMA) technique. This method was used because of its great advantages for industrial applications (reducing time process, solid preform, large scale production . . .). The structures and phase's homogeneity of alloying compounds were analyzed by several experimental measurements.

The hydrogen absorption properties are presented at 350 ° C. Samples $X = 50$ and 58.6 show a maximum hydrogen capacity of 3.5 and 3.7 wt%, respectively. For these two compounds, the pressure–composition isotherm (PCT) curves show two absorption plateaux, with equilibriums around 10 bar which are higher than that of pure MgH_2. The shape discontinuity corresponds to the transformation of γ-$Mg_{17}Al_{12}$ to MgH_2 and to the intermediate β-Al_3Mg_2 phase, before the completed decomposition in MgH_2 hydride and pure Al-fcc in a second step. After final desorption, the initial compounds are recovered, indicates that the reactions are reversible. These behaviors are confirmed by X-ray diffraction (XRD) patterns refined by the Rietveld method.

Keywords: Intermetallics; Metal hydrides; Gas–solid reactions; Mechanical alloying; Crystal structure; Phase diagrams

1. Introduction

Among the light weight absorbing materials of high hydrogen capacity, magnesium is one of the most attractive compounds [1], but its H-related applications are limited, particularly because of its slow sorption reactions (recent progress about kinetics are reviewed in Refs. [2,3]). Some additive elements can form Mg-based alloys and modify its initial hydrogenation thermodynamic properties. For example, Mg_2Ni is a promising H-storage alloy with weight H-content higher than 3 wt% [4]. Since the melting temperature of Mg and Ni differ much, special precautions are indispensable to adjust the alloy composition to the desired value [5]. A good method for alloying is the ball milling (BM): the mechanical energy serves as the driving force to form nanocrystalline compounds from the powders (See the review [6] for more details).

Aizawa et al. have been developing the bulk mechanical alloying (BMA) procedure as a new alternative to yield various nano-structured materials [7]. Different from the conventional milling methods, the BMA technique is based on the repeated forging processes of extrusion–compaction cycles within one-fiftieth of the process time reported in conventional BM type. As the example of synthesizing the Mg_2Ni single phase, it should be mentioned that 2000 BMA cycles correspond to 4.4 h of processing time [8], which is much shorter than the conventional BM type, i.e. about 200 h. This could be a great advantage of BMA for industrial applications in high productivity. In addition to the reduction of time duration for alloying, the other advantages are obtaining a solid preform of

* Corresponding author.
E-mail addresses: jc.crivello@gmail.com (J.-C. Crivello), tkuji@urchin.fc.u-tokai.ac.jp (T. Kuji).

0925-8388/$ – see front matter © 2007 Elsevier B.V. All rights reserved.
doi:10.1016/j.jallcom.2006.12.055

dense compact powder and reducing the surface exposure to oxidation.

In the present work, a study on the binary Mg–Al system toward hydrogenation is presented. The Mg–Al phase diagram shows different intermetallics phases [12] in which the stable β- and γ-phases have a negative enthalpy of mixing and could be obtain by congruent transformation. This feature combined with the low cost of magnesium and aluminum suggests an excellent potential for hydrogen-related applications. The first investigation of this system began in 1974 [9], but at present the complex hydrogenation process is not clearly identified and presents some contradictory results [10,11]. Considering the $Mg_{17}Al_{12}$and $Mg_{50}Al_{50}$compounds, the hydrogen absorption properties at 350 ° C are presented in this paper. The transformation and evolution of the initial Mg–Al structures were discussed considering the formation after BMA treatments, post-annealing, and following the hydrogenation–dehydrogenation cycles.

2. Experimental details

The Mg_XAl_{100-X} system is investigated at two nominal compositions: one at the ideal γ-phase composition ($X = 58.62$, usually given as $Mg_{17}Al_{12}$ despite its large solubility range at high temperatures) and one other at 50% of each element Mg–Al. More compositions are studied in a previous paper where the extend homogeneity range of the γ-phase is investigated from $X = 47.5$ to 70 [13]. The two present compounds are elaborated by BMA process at the Research Center for Advanced Science and Technology, University of Tokyo. Details of this technique, synthesizing process and influence of cycles numbers has been described earlier [14–16].

After milling, each sample was heated in a stainless reactor at 350 ° C for 12 h under vacuum. This temperature is about 100 ° C less than the liquidus and was also chosen for the hydride formation analyzes. The pressure–composition isotherm (PCT) has been determined using Sieverts technique. For the initial activation, several hydrogenation–dehydrogenation cycles were made before starting the PCT measurements. The equilibrium pressure was determined within the accuracy of 7×10^{-2} bar below 7 bar and 1.0% of reading above.

The differential scanning calorimetry (DSC) measurements were performed with a Rigaku DSC-8230 instrument with flowing pure argon gas and a heating rate of 10 ° C/min. The powders were characterized by X-ray diffraction (XRD) MAC science MXP^3 with Cu Kα radiation at 40 kV–30 mA settings and 2θ from 10° to 120°. The resulting profiles were analyzed with the Rietveld refinement program Fullprof [17].

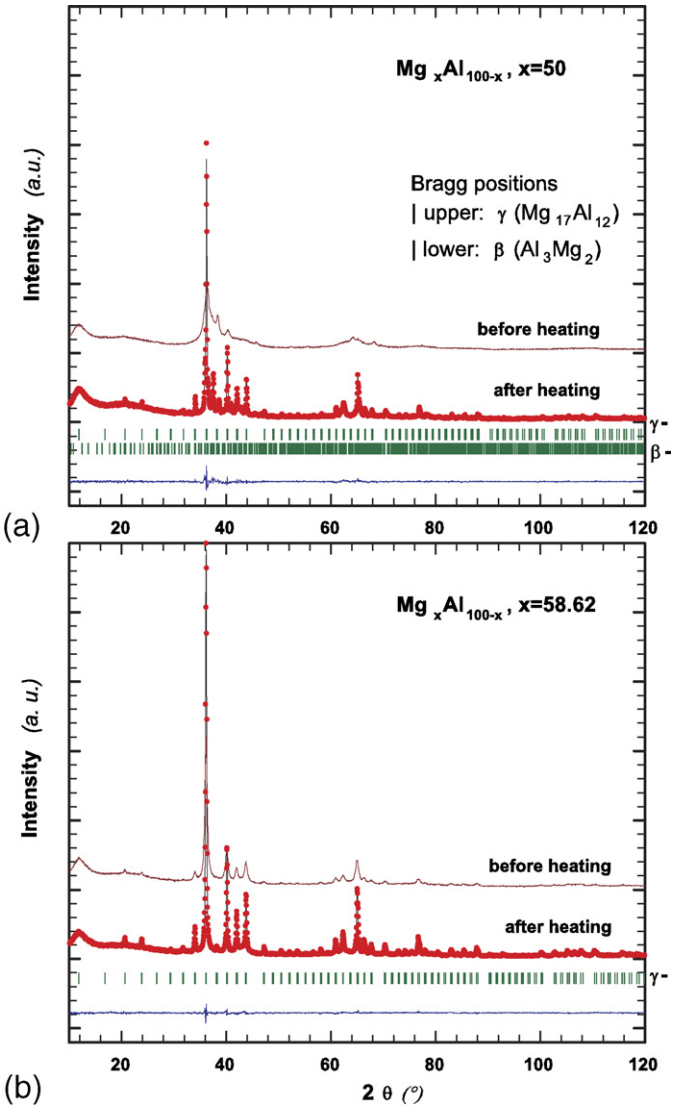

Fig. 1. Observed (points), calculated (line) and difference (bottom line) XRD powder diffraction patterns of Mg_XAl_{100-X} for (a) the $X = 50$ compound and (b) the ideal composition $Mg_{17}Al_{12}$ ($X = 58.62$). The pattern of the compound before heating is also represented by a line shifted above. The Bragg positions of the γ-phase (upper) and β-phase (lower) are indicated by vertical bars with legend on the right scale.

3. Results and discussion

3.1. Synthesis of the compounds

The XRD results were presented before and after annealing in Fig. 1. They show many differences for the two samples.

Table 1
Structure refinement results from X-ray diffraction patterns of $Mg_XAl_{100-X}$for the ideal composition $Mg_{17}Al_{12}$, $X = 58.6$ and the $X = 50$ compound

$X = 58.6$, $Mg_{17}Al_{12}$
Phase: γ-$Mg_{17}Al_{12}$, α-Mn (A12) structure $I43m$ (217), $a = 10.5295(2)$ Å, $R_{Bragg} = 4.2\%$
$R_p = 11.6\%$, $R_{wp} = 10.2\%$, $\chi^2 = 1.57$
$X = 50$
Phase 1: γ-$Mg_{17}Al_{12}$, α-Mn (A12) structure $I43m$ (217), $a = 10.5101(3)$ Å, $R_{Bragg} = 4.99\%$
Phase 2: β-Al_3Mg_2, β-phase structure [18] $Fd\bar{3}m$ (227), $a = 28.2289(9)$ Å, $R_{Bragg} = 15.7\%$
$R_p = 20.3\%$, $R_{wp} = 15.3\%$, $\chi^2 = 2.02$; phase refined contents: (1) ∼ 68.2%, (2) ∼ 31.8%

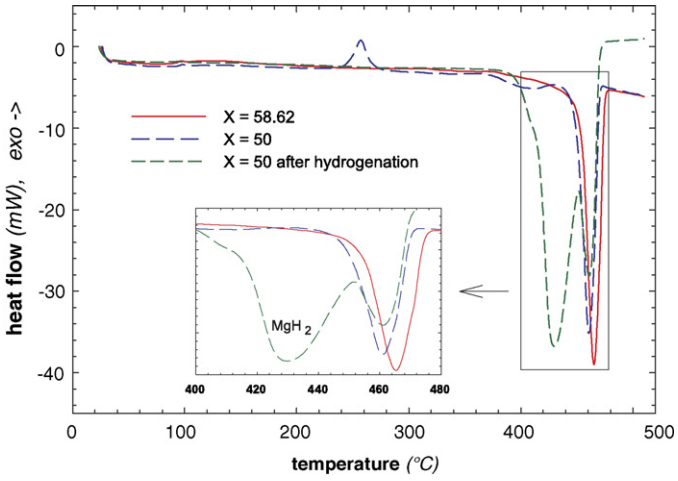

Fig. 2. DSC traces from 18 mg of powder of Mg_XAl_{100-X} for the ideal composition $Mg_{17}Al_{12}$, $X = 58.6$ and the $X = 50$ compound before and after absorption process.

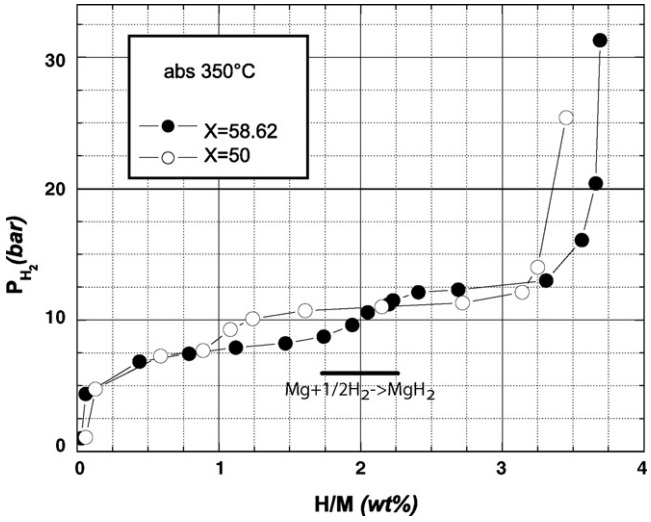

Fig. 3. PCT absorption curves at 350 ° C of Mg_XAl_{100-X} for the ideal composition $Mg_{17}Al_{12}$, $X = 58.6$ and the $X = 50$ compound.

Whereas, the compound at initial composition $X = 50$ needs a post-annealing to complete its well crystallization, the one at the ideal $Mg_{17}Al_{12}$ composition forms the single γ-phase just after the BMA process (Table 1, α-Mn structure detailed in a previous paper [13]). The Rietveld refinement shows that the $Mg_{50}Al_{50}$compounds is composed of two phases: the γ-phase and the β-phase (Al_3Mg_2). We had considered the β-phase as the complex cubic structure described elsewhere [18]. In order to investigate the homogeneity of present phases, thermal DSC measurements have been made. The DSC traces from 18 mg of powder for the two nominal compositions, after BMA alloying and before annealing, are presented in Fig. 2. The compound at the ideal composition $Mg_{17}Al_{12}$shows an endothermic peak at 465 ° C, corresponding to the melting point. For $X = 50$, the melting point is localized near to the same temperature ($T = 460$ ° C). A new exothermic peak appears caused by the formation of new complex phases at $T = 257$ ° C. After annealing, this peak disappears in conjunction with the better crystallization of the structure (corresponding DSC trace not shown).

Results of thermal and structural properties are quite in agreement with the binary phases diagram [12].

3.2. Hydrogen absorbing properties

After the activation of the two samples, the PCT of hydrogen absorption were determined at 350 ° C. The PCT curves are presented in Fig. 3 and reveal the following characteristics:

- At this temperature, the maximum rate of hydrogen absorption capacity for $X = 50$ and 58.6 are, respectively, obtained at $H/M_{max} = 3.5$ and 3.7 wt% (0.92 and 0.97 H/M *normalized*).
- Two sloping plateaux are observed, indicating that the hydride formation is realized in a two-step process. The inflexion points are localized at $H/M_{ifx} \simeq 1.1$ and 2.1 wt%, respectively, for $X = 50$ and 58.6.
- Half-plateau equilibrium pressures of the first plateau are very close: $P^1_{X=50} \simeq 7.3$ bar and $P^1_{X=58.6} \simeq 7.9$ bar. The second plateau are also situated at a similar pressure for the two samples ($P^2_{X=50} \simeq 11.3$ bar and $P^2_{X=58.6} \simeq 12.3$ bar). Considering the accuracy of the experimental measures, the small pressure difference could be slight, specially in the lower plateau. According to this approximation, the two absorption plateaux suggest to be associated to the same hydride formation for the two samples.

For these two compositions compared to Mg–H_2 system, we conclude that the addition of Al leads to a decrease of the maximum hydrogen capacity and to an increase of their plateaux pressures, both higher than the equilibrium pressure of the MgH_2 hydride at the same temperature [19]. These characteristics suggest that the Al-content controls the thermodynamic characteristics by the formation of Mg-based hydride as we will show in the next section.

3.3. Discussion of the two-step hydride formation

From the $Mg_{17}Al_{12}$composition, Bouaricha et al. had reported its present hydrogenation into two decompositions with a first equation including *y*, a variable dependant on the various proportion of phases [20]. Considering that the first step leads to transform all the Al atoms from γ- to β-phase, no pure Al-fcc should be formed in the first reaction. In this case, the hydrogen absorption is described into the two simplified following equations:

$$Mg_{17}Al_{12} + 9H_2 \rightleftarrows 9MgH_2 + 4Al_3Mg_2 \quad (*2.40\,wt\%) \qquad (1)$$

$$4Al_3Mg_2 + 8H_2 \rightleftarrows 8MgH_2 + 12Al \quad (*2.04\,wt\%) \qquad (2)$$

If we consider the completed decomposition of Mg-based compounds to form MgH_2hydride (Eqs. (1) + (2)), the maximum absorption rate expected should be $H/M^*_{max} = 17 \times 2\,H/M$ by f.u $= 1.17\,H/M\,normalized = 4.44$ wt%. After the

Table 2
Structure refinement results from X-ray diffraction patterns of the ideal composition $Mg_{17}Al_{12}$ (Mg_XAl_{100-X}, $X = 58.6$) during hydrogenation

(a) At complete absorption state
Phase 1: Hydride α-MgH_2, $a = 4.5120(2)$ Å, $c = 3.0179(2)$ Å, $R_{Bragg} = 6.54\%$
Phase 2: Al-fcc, $a = 4.0520(2)$ Å, $R_{Bragg} = 4.67\%$
$R_p = 27.0\%$, $R_{wp} = 17.3\%$, $\chi^2 = 1.84$
(b) At partial desorption state H/M ≃ 3 wt%
Phase 1: Hydride α-MgH_2, $a = 4.5137(3)$ Å, $c = 3.0179(3)$ Å, $R_{Bragg} = 6.92\%$
Phase 2: Al-fcc, $a = 4.0731(3)$ Å, $R_{Bragg} = 8.93\%$
Phase 3: β-Al_3Mg_2, β-phase structure [18] $a = 28.224(2)$ Å, $R_{Bragg} = 12.9\%$
$R_p = 24.9\%$, $R_{wp} = 25.0\%$, $\chi^2 = 4.02$
(c) At partial desorption state H/M ≃ 1 wt%
Phase 1: Hydride α-MgH_2, $a = 4.5130(9)$ Å, $c = 3.016(1)$ Å, $R_{Bragg} = 15.4\%$
Phase 2: β-Al_3Mg_2, β-phase structure [18] $a = 28.220(2)$ Å, $R_{Bragg} = 26.2\%$
Phase 3: γ-$Mg_{17}Al_{12}$, α-Mn (A12) structure $a = 10.5020(4)$ Å, $R_{Bragg} = 8.90\%$
$R_p = 37.1\%$, $R_{wp} = 23.4\%$, χ^2 =1.34
(d) After complete desorption
Phase: γ-$Mg_{17}Al_{12}$, α-Mn (A12) structure $a = 10.4970(3)$ Å, $R_{Bragg} = 9.57\%$
$R_p = 25.7\%$, $R_{wp} = 19.8\%$, $\chi^2 = 3.11$

first reaction Eq. (1), the inflexion point should be $H/M^*_{ifx} = 2.40$ wt%. These expected values may be overestimated but are close to the experimental measurements.

For $X = 58.6$, we can precisely confirm the decomposition by using the Rietveld refinements (Table 2). Associated XRD patterns are shown in Fig. 4, corresponding to the compounds after the completed absorption (Fig. 4a), two partial desorptions (H/M ≃ 3 and 1 wt%, in Fig. 4 b and c), and after the full desorption of hydrogen (Fig. 4d).

In the case of the completed absorption, the formation of the magnesium hydride MgH_2 has been found with the presence of Al-fcc. After the full desorption, the analysis shows only the presence of the single γ-$Mg_{17}Al_{12}$ phase. Thus, (1) and (2) reactions are totally reversible and the initial compound is recovered. Considering the two partial results from the two different plateau pressures (H/M ≃ 3 and 1 wt%), the Rietveld refinements confirm that the γ-$Mg_{17}Al_{12}$ compound is partially decomposed into the intermediary β-Al_3Mg_2 before the completed formation of MgH_2 hydride and pure Al. The two partial hydrogenation samples show the same results from absorption or desorption states. In fact, it was verified that the PCT desorption curves present also two plateaux (figure not shown).

All of these results are self-consistent with the two equations of transformation (1) and (2) proposed above.

Before hydrogenation, the compound with 50% of each Mg–Al element is initially composed of the two γ- and β-phases, with refined contents of about 70–30% (Table 1). However, the behaviors toward hydrogen are similar: after full absorption, the sample is composed of MgH_2hydride with Al-fcc and is recovered after desorption (figures not shown). As a result, the first plateau of absorption corresponds to the formation of MgH_2 and complements the transformation of the initial 30%

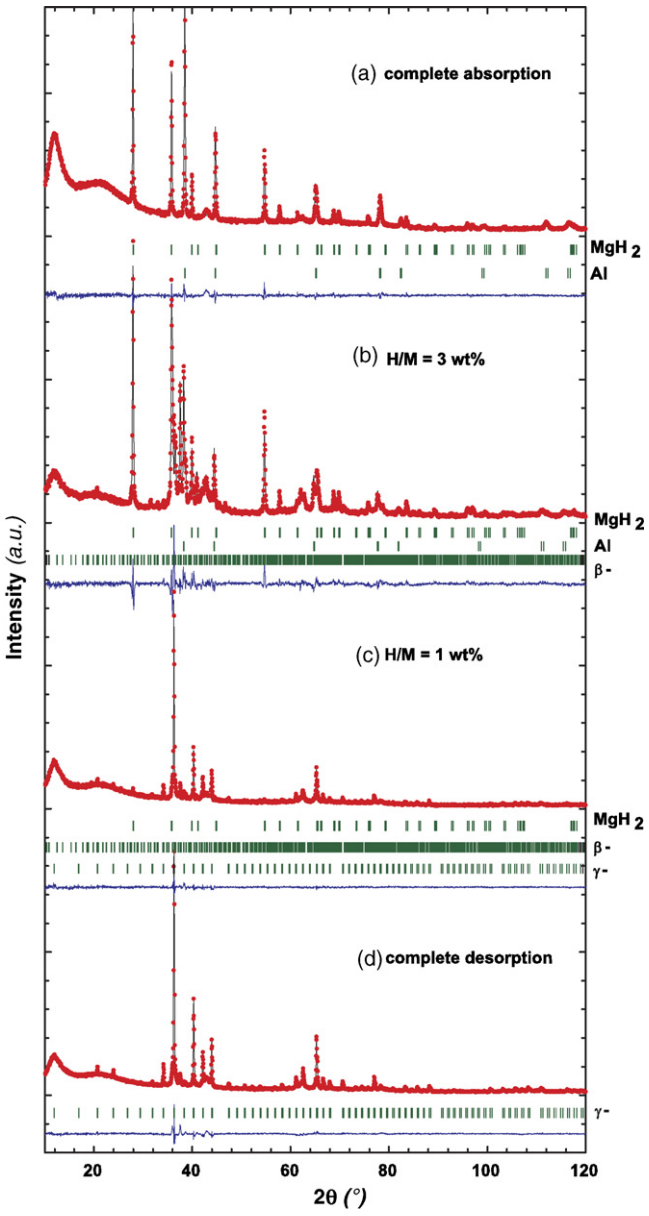

Fig. 4. Observed (points), calculated (line) and difference (bottom line) XRD powder diffraction patterns of the ideal composition $Mg_{17}Al_{12}$ (Mg_XAl_{100-X}, $X = 58.62$) during hydrogenation, from top to bottom: (a) at the completed absorption state, at the partial desorption state (b) H/M ≃ 3 wt%, (c) H/M ≃ 1 wt% and (d) after full desorption. The different Bragg positions are indicated by vertical bars with legend on the right scale.

β-Al_3Mg_2. In this way, the first plateau pressure is similar but ends before the $X = 58.6$ compound. In considering that the second plateau of hydride formation is associated to the same reaction of transformation (2), the Mg resulted from Al_3Mg_2will form the Mg-hydride and Al-fcc. That is why the second plateau is longer for $X = 50$: $MgH_2$is mainly formed during reaction (2) from the fact that the β-phase is more abundant; it comes from the initial composition and after the transformation (1).

Reaction (2) has already been presented: H reacts with single β-Al_3Mg_2 phase by the same decomposition $1/2\,Al_3Mg_2 + H_2 \rightleftarrows MgH_2 + 3/2\,Al$. This reaction was reported from a sin-

gle plateau of the PCT curves at 300–385 ° C by Fernández et al. [21] and beyond 375 ° C by Mintz et al. [22].

In Fig. 2, the DSC specter confirms the XRD results: the trace of the 50% sample after hydrogenation shows the endothermic peak of the melting point at the same temperature than before hydrogenation and without interactions with the β-phase at $T = 257$ ° C. However, a huge peak around 430 ° C is found, which is corresponding to the desorption of the MgH_2 hydride.

These present results are in agreement with previous reports [20,23]: each metastable Mg–Al phase has its own thermodynamic characteristics for the formation of $MgH_2$and for each transformation, the equilibrium pressure of hydride formation are shifted toward higher pressures as compared to the standard reaction $Mg + H_2 \rightarrow MgH_2$.

4. Conclusions

In this paper, we have shown that compounds which contain the γ-$Mg_{17}Al_{12}$phase are decomposed in the MgH_2 hydride and pure Al after the completed hydrogen absorption. According to the presence of two plateau pressures and the Rietveld refinements, we concluded that the hydrogenation is realized in a two-step process. At first, the γ-$Mg_{17}Al_{12}$ phase forms the intermediary β-Al_3Mg_2. From the latter, the hydrogen leads to finish the formation of the hydride MgH_2 in the second step. These reactions are reversible. No Al-based hydride is formed, but considering the desorption process, it is clear that Al has found to destabilize MgH_2 by forming the two Mg–Al alloys as it was suggested by Vajo et al. [24].

In the Mg_XAl_{100-X}–H_2system, the proportion of initial Al-based phases should be the key factor which controls the thermodynamics properties of hydrogenation. This study will continue with the measurement of the hydride formation enthalpy relating to each plateau. The hydrides microstructure will be specifically analyzed in order to better understand the hydrogenation process. In order to generalize this behavior, more X compositions in Mg_XAl_{100-X} alloys will also be investigated.

Acknowledgements

This work was supported financially by the Japan NEDO project (New Energy and Industrial Technology Development Organization) and the French Ministry for Foreign Affairs. Prof. Kondoh of Research Center for Advanced Science and Technology, University of Tokyo, is acknowledged for his support in the instrumental BMA process.

References

[1] B. Bogdanović, T.H. Hartwig, B. Spliethoff, Int. J. Hydrogen Energy 18 (1993) 575–589.
[2] M. Dornheim, N. Eigen, G. Barkhordarian, T. Klassen, R. Bormann, Adv. Eng. Mater. 8 (2006) 377–385.
[3] T.R. Jensen, A. Andreasen, T. Vegge, J.W. Andreasen, K. Ståhl, A.S. Pedersen, M.M. Nielsen, A.M. Molenbroek, F. Besenbacher, Int. J. Hydrogen Energy 31 (2006) 2052–2062.
[4] J.J. Reilly, R.H. Wiswall, Inorg. Chem. 7 (1968) 2254–2256.
[5] J. Huot, G. Liang, R. Schulz, Appl. Phys. A 72 (2001) 187–195.
[6] C. Suryanarayana, Prog. Mater. Sci. 46 (2001) 1–184.
[7] T. Aizawa, K. Tatsuzawa, J. Kihara, Mechano-metallurgical processing for direct fabrication of solid non-equilibrium phase materials, J. Fac. Eng. Univ. Tokyo XLII 42 (N3) (1993) 261–279.
[8] T. Aizawa, T. Kuji, H. Nakano, J. Alloys Compd. 291 (1999) 248–253.
[9] J.J. Reilly, R.H. Wiswall, C.H. Waide, Report TEC-75/001, U.S. Energy Research and Development Admin., 1974, 84 pp.
[10] M. Bououdina, Z.X. Guo, J. Alloys Compd. 336 (2002) 222–231.
[11] Q.A. Zhang, H.Y. Wu, Mater. Chem. Phys. 94 (2005) 69–72.
[12] J.L. Murray, Bull. Alloy Phase Diagr. 3 (1982) 60–74.
[13] J.C. Crivello, T. Nobuki, T. Kuji, Intermetallics 15 (2007) 1432–1437.
[14] H. Yabe, T. Kuji, J. Metastable Nanocryst. Mater. 24–25 (2005) 173–176.
[15] H. Yabe, T. Kuji, J. Alloys Compd., in press.
[16] T. Nobuki, J.-C. Crivello, T. Kuji, Proceedings of the 110th Conference of Japan Institute of Light Metals, Kitakyushu, Japan, 2006, p. 121.
[17] J. Rodríguez-Carvajal, Proceedings of the XVth Congress of International Union of Crystallography, Satellite Meeting on Powder Diffraction, Toulouse, France, 1990, p. 127.
[18] S. Samson, Acta Cryst. 19 (1965) 401–413.
[19] J.F. Stampfer, C.E. Holley, J.F. Suttle Jr., J. Am. Chem. Soc. 82 (1960) 3504–3508.
[20] S. Bouaricha, J.P. Dodelet, D. Guay, J. Huot, S. Boily, R. Schulz, J. Alloys Compd. 297 (2000) 282–293.
[21] J.F. Fernández, F. Leardini, J. Bodega, J.M. Joubert, F. Cuevas, M. Baricco, M. Di Chio, H. Figiel, M. Feuerbacher, J. Alloys Compd., in this issue.
[22] M.H. Mintz, Z. Gavra, G. Kimmel, Z. Hadari, J. Less-Common Met. 74 (1980) 263–270.
[23] A. Zaluska, L. Zaluski, J.O. Ström-Olsen, Appl. Phys. A 72 (2001) 157–165.
[24] J.J. Vajo, F. Mertens, C.C. Ahn, R.C. Bowman, B. Fultz Jr., J. Phys. Chem. B 108 (2004) 13977–13983.